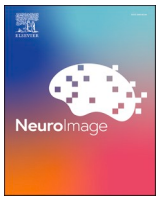
NeuroImage 321 (2025) 121540



Contents lists available at ScienceDirect

NeuroImage

journal homepage: www.elsevier.com/locate/ynimg





Structural-Functional Brain Network Modulation using Transcranial Focused Ultrasound Stimulation: Implications on the Default Mode Network in Humans

Chang-hyun Park [a,1], Song E. Kim [b,d,1], Yun Seo Choi [b,d,e], Jihye Lee [b,f], Seo Young Lee [a], Ju Hyeong Kang [a], Seongeun Hwang [g], Young Goo Kim [c,d], Hyang Woon Lee [a,b,d,f,*]

[a] Artificial Intelligence Convergence Graduate Program, Ewha Womans University, Seoul, South Korea
[b] Department of Neurology, College of Medicine, Ewha Womans University, Seoul, South Korea
[c] Department of Neurosurgery, College of Medicine, Ewha Womans University, Seoul, South Korea
[d] Department of Medical Science, College of Medicine, Ewha Womans University, Seoul, South Korea
[e] Convergence Medical Research Institute, Ewha Womans University Mogdong Hospital, Seoul, South Korea
[f] Computational Medicine, Graduate Program of System Health Science and Engineering, Ewha Womans University, Seoul, South Korea
[g] Department of Neurology, Ewha Womans University Mogdong Hospital, Seoul, South Korea

ARTICLE INFO

Keywords:
Transcranial focused ultrasound
Medial prefrontal cortex
Default mode network
Structure-function correspondence
Neuromodulation

ABSTRACT

Transcranial focused ultrasound (tFUS) has emerged as a promising noninvasive technique for brain stimulation due to its precise focusing and deep penetration capabilities. However, its potential to modulate brain networks beyond the stimulation site and optimal sonication parameters required for such modulation remain unclear. In light of this knowledge gap, this study investigates the effects of tFUS targeted at the medial prefrontal cortex (mPFC), a key component of the default mode network (DMN), to determine whether varying the sonication parameters could specifically modulate the DMN. Specifically, in this study, 21 healthy participants were divided into groups that received excitatory, suppressive, or sham tFUS stimulation targeting the mPFC. To assess the effects, diffusion-weighted MRI and resting-state functional MRI were employed to assess the correspondence between structural and functional brain connectomes before and after tFUS. Subsequently, changes following tFUS were compared among the three groups. Our results showed that while tFUS generally increased coupling between structure and function near the stimulation site after both excitatory and suppressive stimulation, a significant enhancement in structure–function correspondence was specifically observed within the DMN connected to the stimulation site under excitatory stimulation. Based on these observations, the findings highlight the potential of specific tFUS protocols to effectively modulate the DMN, thereby offering insights into optimizing tFUS for brain network modulation and its potential as a non-invasive therapeutic intervention.

1. Introduction

The recent surge in human ultrasound neuromodulation research has led to the development of technologies for focusing ultrasound through the human skull (Clement and Hynynen, 2002). Ultrasound stimulation is theoretically known to target deep brain structures with high spatial resolution (Kubanek, 2018), which represents distinct advantages over electromagnetic neuromodulation technologies such as transcranial magnetic stimulation or transcranial direct current stimulation (Beisteiner, 2022). Low-intensity transcranial focused ultrasound (tFUS) has been investigated in neuromodulation studies in both humans and other animals during the past decade, showing promising results in inducing alterations in brain functions and associated behavioral changes.

The potential of tFUS has been substantiated through its application to various brain regions, including cortical areas such as the motor, somatosensory, and visual cortices, as well as subcortical areas such as the thalamus, globus pallidus, and substantia nigra, demonstrating both excitatory and inhibitory effects depending on the targeted brain region and the sonication parameters (for reviews, see (Sarica et al., 2022;

* Corresponding author.
E-mail address: leeh@ewha.ac.kr (H.W. Lee).
[1] These authors equally contributed to this work as co-first authors.

https://doi.org/10.1016/j.neuroimage.2025.121540
Received 30 November 2024; Received in revised form 1 August 2025; Accepted 16 October 2025
Available online 17 October 2025
1053-8119/© 2025 The Authors. Published by Elsevier Inc. This is an open access article under the CC BY-NC license (http://creativecommons.org/licenses/by-nc/4.0/).

Zhang et al., 2021)). Moreover, safety concerns regarding tFUS have been considered minimal, as evidenced by studies in humans using various ultrasound parameters (Legon et al., 2020). The minimal safety concerns associated with tFUS strengthen its potential as a therapeutic intervention for various disorders. This technology has already been suggested to be effective in conditions such as chronic pain (Monti et al., 2016), Alzheimer's disease (Beisteiner et al., 2020), depression (Reznik et al., 2020), and epilepsy (Stern et al., 2021). Furthermore, concerns about the safety of tFUS have been deemed mnimal, as evidenced by studies in humans using different sonication parameters (Legon et al., 2020). The minimal safety concerns associated with tFUS bolster its potential as a therapeutic intervention for a variety of disorders. This technique has already been suggested to offer benefits for disorders such as chronic pain (Monti et al., 2016), Alzheimer's disease (Beisteiner et al., 2020), depression (Reznik et al., 2020; Oh et al., 2024), and epilepsy (Stern et al., 2021).

Nonetheless, the transition of tFUS from an experimental tool to a standard method in neuroscience and clinical practice is still ongoing. One critical unresolved question is the extent to which tFUS , targeting specific brain regions, can induce measurable changes or modulate brain circuits. Additionally, the nature and extent of the modulation induced by tFUS are currently understood to vary depending on the sonication parameters used, but standard parameters have not yet been established. Addressing those research gaps is crucial for advancing tFUS from a promising technique to a standard tool in neuroscience research and clinical practice.

Therefore, we administered tFUS to the medial prefrontal cortex (mPFC), using different sonication parameters that are thought to have excitatory or suppressive effects, which is involved in self-referential thinking and emotional regulation. The mPFC is a crucial component of the default mode network (DMN), together with the medial and/or lateral parietal, and medial and/or lateral temporal cortices (Raichle, 2015). The DMN is thought to play a mechanistic role in human cognition (Smallwood et al., 2021), such that alterations in the DMN have been associated with various neuropsychiatric disorders (for reviews, see (Broyd et al., 2009; Mohan et al., 2016)). In this study, we examined whether we could induce specific modulation of the DMN by targeting tFUS to the mPFC, and tested different sonication parameters to determine which one would effectively induce the desired modulation.

To assess the efficacy of tFUS in modulating brain circuits beyond the mPFC, we measured changes in brain structure–function correspondences after tFUS. Brain structure–function correspondence analyses have shown promising results in decoding brain states, such as between tasks (Griffa et al., 2022), and in detecting changes in the brain state, such as after short-term learning (Park et al., 2024), by accounting for the underlying brain structure in which brain function is manifested. Based on the specificity of brain structure–function correspondences and brain states, we hypothesized that different brain states before and after tFUS could be discriminated by changes in brain structure–function correspondences in the mPFC and surrounding brain areas.

2. Material and methods

2.1. Participants

For this study, right-handed individuals aged 45 to 65 years without any neurological or psychiatric conditions, significant cognitive issues, contraindications of MRI, or certain physical impediments were recruited. The study was stringent in excluding those with specific brain or scalp conditions that could interfere with ultrasound treatment, as well as people who were pregnant or breastfeeding. Based on these criteria, 21 participants (age = 54.4 ± 6.0 years; 9 males, 12 females; all East Asians) were included in the study. Written informed consent was obtained from all participants in accordance with the Declaration of Helsinki and its later amendments, and the study was approved by the Institutional Review Board of Ewha Womans University Mokdong Hospital (EUMC 2019–12–013).

2.2. tFUS administration

For each individual, baseline multimodal brain imaging of computed tomography (CT) and MRI was conducted one week before we administered tFUS, which was applied using an NS-US100 system (Neurosona, Seoul, Korea) approved by the Ministry of Food and Drug Safety of Korea. The tFUS system used a single-element transducer (80 mm diameter, 68 mm focal length) that produces a cigar-shaped focus of approximately 9 mm in diameter and 50 mm in length. The system does not allow individual adjustments of the sonication focus size, but adjustments to the depth of focus were made using compressible hydrogels. The baseline neuroimaging was used to exclude those with substantial brain calcifications or enlarged frontal sinuses, which could obstruct the ultrasound pathway, and to locate the ultrasound focus on the mPFC with an image-guided navigation system.

Four PinPoint donut-shaped, self-adhesive markers (Beekley Corp., Bristol, CT, USA) placed behind the bilateral ears and above the bilateral eyebrows provided stable reference points for the image-guided navigation system, ensuring consistent anatomical co-registration across sessions. A detailed visualization of the MRI-specific experimental paradigm is presented in Fig. 1, while comprehensive details of the tFUS setup, including the experimental protocol and acoustic profile, can be found in our previous publication (Kim et al., 2022).

For this single-blind, randomized controlled trial, participants were divided into three groups receiving excitatory, suppressive, or sham tFUS stimulation. The distinction between excitatory and suppressive protocols were summarized in Table 1 and Fig. 2. The excitatory and suppressive protocols shared an operating frequency of 250 kHz, a pulse duration (PD) of 0.5 msec and a pulse train duration (PTD) of 300 msec. The excitatory stimulation was characterized by a 70 % duty cycle (DC), with a pulse repetition frequency (PRF) of 1400 Hz, a pulse repetition interval (PRI) of 0.714 msec, and a 5-*sec* inter-pulse train interval (Fig. 2A), while the suppressive stimulation featured a 5 % DC, with a PRF of 100 Hz, a PRI of 10 msec, and continuous pulsing with no inter-pulse train interval (Fig. 2B). The spatial-peak pulse-average intensity (I_{sppa}) was reported as $I_{sppa} = 0.75$ W/cm^2 for both stimulations, and the spatial-peak temporal-average intensity (I_{spta}) was I_{spta} = 525 vs. 38 mW/cm^2 for the excitatory and suppressive stimulations, respectively, which were determined based on acoustic calibration and following the International Transcranial Ultrasonic Stimulation Safety and Standards Consortium (ITRUSST) guidelines (Martin et al., 2024). The higher energy delivery in the excitatory stimulation was designed to modulate neural excitability, while the reduced energy in the suppressive stimulation was intended to produce inhibitory effects, based on a lower duty cycle (Dell'Italia et al., 2022). These parameters were selected to achieve effective neuromodulation while minimizing potential mechanical or thermal sensory confounds.

2.3. MRI data collection

MRI data were collected using a 3T Achieva scanner (Philips Healthcare, Best, Netherlands). Diffusion-weighted MRI (dMRI) data composed of 33 vol images, 32 with diffusion weighting at a *b* value of 1000 s/mm^2 and one without diffusion weighting, were acquired with the following parameters: number of slices = 70, slice thickness = 2.00 mm, matrix size = 128 × 128, and in-plane resolution = 1.7 mm × 1.72 mm. Resting state functional MRI (fMRI) data consisting of 220 vol images were acquired every 2 s with the following parameters: number of slices = 35, slice thickness = 3.50 mm, matrix size = 64 × 64, and in-plane resolution = 3.44 mm × 3.44 mm. T1-weighted structural MRI (sMRI) data composed of one volume image were acquired with the following parameters: number of slices = 320, slice thickness = 0.50 mm, matrix size = 480 × 480, and in-plane resolution = 0.50 mm × 0.50

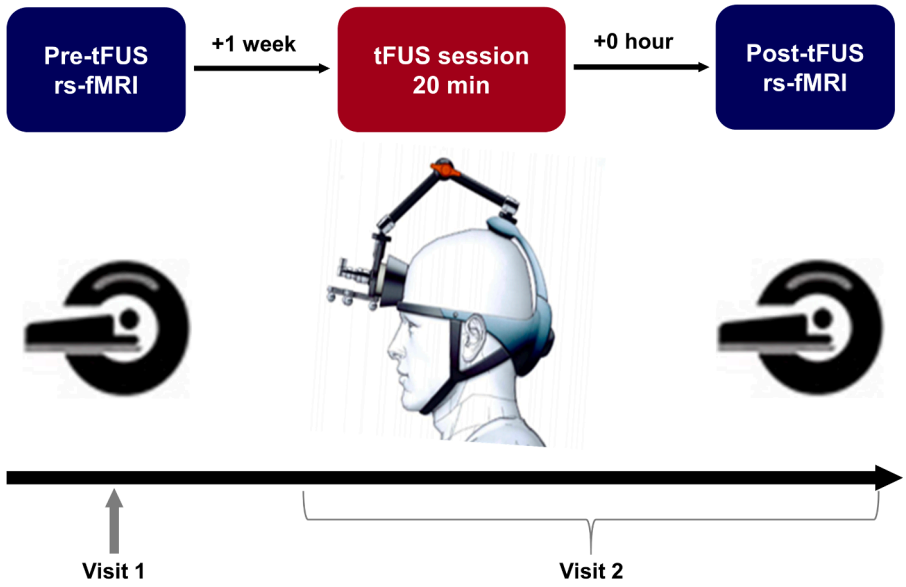


Fig. 1. Schematic diagram of the study design, including the schedule for MRI acquisition and transcranial focused ultrasound (tFUS). The pre-tFUS MRI was obtained at Visit 1, one week prior to tFUS, and post-tFUS MRI was performed at Visit 2, immediately after the 20-min tFUS session. Each MRI session (~30 min) included structural and resting-state functional MRI sequences.

Table 1
Summary of stimulation parameters for excitatory and suppressive transcranial focused ultrasound.

Stimulation parameters	Excitatory	Suppressive
Operating frequency	250 kHz	250 kHz
Pulse duration (PD)	0.5 msec	0.5 msec
Pulse train duration (PTD)	300 msec	300 msec
Pulse repetition frequency (PRF)	1400 Hz	100 Hz
Pulse repetition interval (PRI)	0.714 msec	10 msec
Duty cycle (DC)	70 %	5 %
Inter-pulse train interval	5 s	0 s (continuous)
Spatial-peak pulse-average intensity (I_{sppa}) in situ	0.75 W/cm^2	0.75 W/cm^2
Spatial-peak temporal-average intensity (I_{spta}) in situ	525 mW/cm^2	38 mW/cm^2

Note: The main pulse timing relationships are PRF = 1/PRI and DC = (PD/PRI) × 100 %. Each pulse train contains 420 pulses (excitatory stimulation) or 30 pulses (suppressive stimulation), with trains repeated at specified intervals over a 20-min session.

mm.

2.4. MRI data preprocessing

We processed the dMRI data using tools in Mrtrix3 (https://www.mrtrix.org/) and FSL (https://fsl.fmrib.ox.ac.uk/fsl/) to correct for artifacts such as motion and eddy current effects and to perform whole brain tractography. Fiber orientation within each voxel was estimated using multi-shell multi-tissue–constrained spherical deconvolution (Jeurissen et al., 2014), leading to whole brain tractography via a probabilistic algorithm based on second-order integration across the fiber orientation distribution (Tournier et al., 2019). This tractography generated 10 streamlines per voxel in a white matter mask, with seeds placed randomly in a voxel. For the resting-state fMRI data, we used tools in SPM12 (https://www.fil.ion.ucl.ac.kr/spm/) for preprocessing, including correction for head motion and spatial smoothing using a Gaussian kernel. To further refine the data, we applied a nuisance covariate regression to account for low-frequency fluctuations, head movements, and non-neuronal signal fluctuations. To achieve transformation between the native spaces of the dMRI and resting state fMRI data and the standard space, we estimated deformation fields for the sMRI data, which had been co-registered to the dMRI and resting state fMRI data in the native spaces.

2.5. fMRI data analysis

While dMRI data were acquired only once before stimulation, resting-state fMRI data were obtained both pre- and post-tFUS, allowing us to compare functional activity and connectivity changes across the three stimulation protocols. Specifically, we measured global signal amplitude (GSA), regional homogeneity (ReHo), and inter-regional functional connectivity (FC). GSA was calculated as the standard deviation of blood oxygen level dependent (BOLD) signals for each voxel, providing a measure of local activity strength. ReHo was computed using Kendall's coefficient of concordance among the time series of each voxel's 27 neighboring voxels, reflecting local signal synchronization. FC was assessed through temporal correlations between BOLD time series of paired brain regions, indicating functional coupling strength. Changes in these metrics between pre- and post-tFUS were calculated across the whole brain and evaluated for differences among the three protocols.

2.6. Brain connectome analysis

For each individual, we constructed a structural connectome from pre-tFUS dMRI data and two functional connectomes from the pre- and post-tFUS resting state fMRI data. We supposed the structural connectome to remain static during the short duration of the tFUS and to serve as the common structural substrate for measuring brain structure–function correspondences pre- and post-tFUS. Using the automated anatomical labeling (AAL) atlas (Tzourio-Mazoyer et al., 2002), which defines 90 cerebral areas in the standard space, the structural connectome was formed by identifying fiber bundles linking pairs of brain areas, and the functional connectomes were based on the signal correlation between pairs of brain areas. That is, the connectomes shared the same nodes (90 brain areas), but they differed in estimating the edges, using fiber bundles for the structural connectome and signal correlation for the functional connectome.

The correspondence between the structural and functional brain connectomes was assessed using the multilinear regression fit between the observed functional connectivity and predicted functional

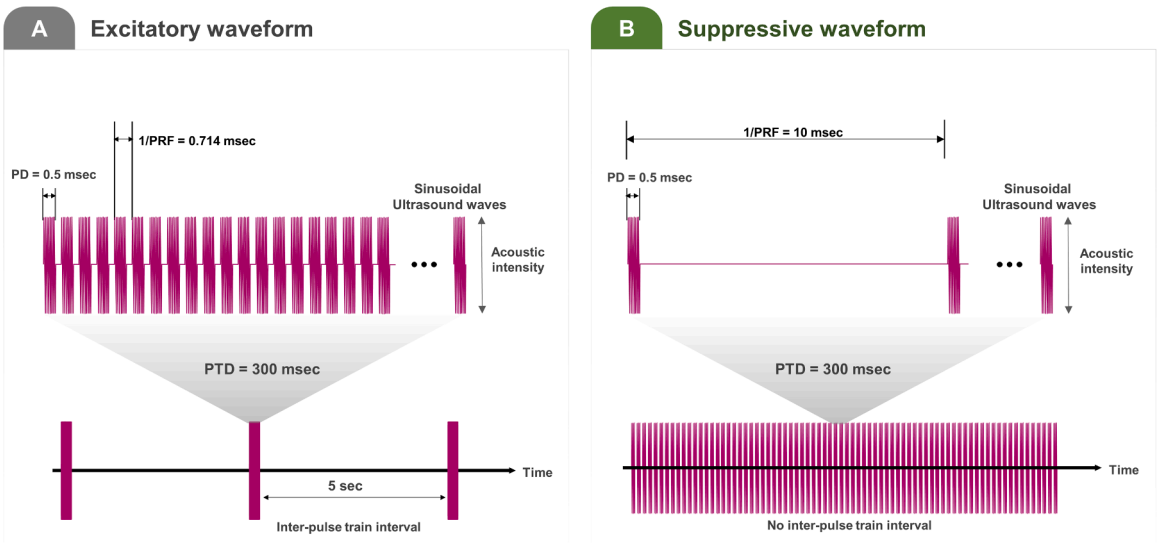


Fig. 2. Comparison of excitatory and suppressive tFUS stimulations for comparative purposes. Schematic representation of focused ultrasound pulse timing parameters for (A) excitatory and (B) suppressive focused ultrasound stimulations, illustrating differences in pulse repetition patterns. PD, pulse duration; PTD, pulse train duration; PRF, pulse repetition frequency.

connectivity, where the prediction of functional connectivity was made using a linear combination of Euclidean distance, path length, and communicability of the observed structural connectivity (Vázquez-Rodríguez et al., 2019). The goodness of fit, as assessed by the coefficient of determination (R^2 value), between the observed and predicted functional connectivity provided the structure–function correspondence at each node.

To elucidate the network-wide implications of tFUS, we explored the involvement of seven cerebral networks, the visual, somatomotor, dorsal attention, ventral attention, limbic, frontoparietal, and default mode networks (Table S1), estimated using functional connectivity profiles across the cerebral cortex (Yeo et al., 2011). The structure–function correspondence across each cerebral network was estimated by averaging the R^2 values of the nodes in that network. The division of the cerebral cortex into the seven networks allowed us to estimate how different networks could be modulated by tFUS applied to the mPFC.

2.7. Statistical analysis

Changes in GSA, ReHo, and FC between pre- and post-tFUS were compared across the three protocols using the Kruskal-Wallis H test. The presence of non-zero changes in structure–function correspondences in each group following tFUS was inferred using the Wilcoxon signed rank test. Pair-wise comparisons of changes among the three groups were made using the Mann-Whitney U test. These statistical inferences were applied at the level of each cerebral network and each node. Although statistically significant results with $p \leq 0.05$ corrected for multiple comparisons using a false discovery rate approach are the primary findings, those with an uncorrected $p \leq 0.05$ are also notable given the limited sample size of this study.

3. Results

3.1. Participant inclusion

Of the total 21 participants with mean age of 54.4 year-old, including 9 males and 12 females, seven were assigned to each stimulation protocol: excitatory stimulation ($n = 7$; age $= 54.9 \pm 6.5$ years; 3 males, 4 females), suppressive stimulation ($n = 7$; age $= 54.3 \pm 6.2$ years; 3 males, 4 females), and sham stimulation ($n = 7$; age $= 54.1 \pm 6.3$ years; 3 males, 4 females). All participants were East Asian, and the age and sex ratio did not differ significantly among the three groups.

3.2. Safety of tFUS administration

During the tFUS procedure, the skin surface temperature was continuously monitored using the system's built-in infrared thermometer and maintained at 35.4 °C, well within the safety limits established by the Ministry of Food and Drug Safety of Korea for the NS-US100 system. This temperature control aligns with established safety protocols for transcranial ultrasound applications (Legon et al., 2020), and was consistent with participants' reports of experiencing no sensation of heating. Additionally, no participants reported auditory confounding or other side effects during or after the procedure, confirming the safety of our stimulation protocols.

3.3. Changes in functional activity and connectivity

Analysis of pre- and post-stimulation resting-state fMRI data revealed distinct trends in GSA, ReHo, and FC across the three experimental conditions. At the whole-brain level, both functional activity and connectivity tended to increase following excitatory stimulation and decrease following suppressive stimulation (Fig. 3). Notably, GSA exhibited a statistically significant difference among the three stimulation protocols. However, when analyzing the changes at the level of the seven cerebral networks, variation was observed across networks, and no network-specific changes reached statistical significance (Figs. S1-S3).

3.4. Node-wise changes in structure–function correspondences

The distribution of structure–function correspondences exhibited different patterns across the cerebral cortex both pre- and post-tFUS (Fig. 4), confirming that structure and function are not uniformly related in the brain (Vázquez-Rodríguez et al., 2019). At the level of each node, changes in brain structure–function correspondences after tFUS with both excitatory and suppressive stimulations were primarily seen as increased coupling between structure and function in the vicinity of the mPFC across the superior frontal gyrus (SFG) (Fig. 5 and Table S2). However, whereas excitatory stimulation elicited changes across broad areas in the SFG, changes surrounding the suppressive stimulation site were confined to the orbital part of the SFG. This pattern

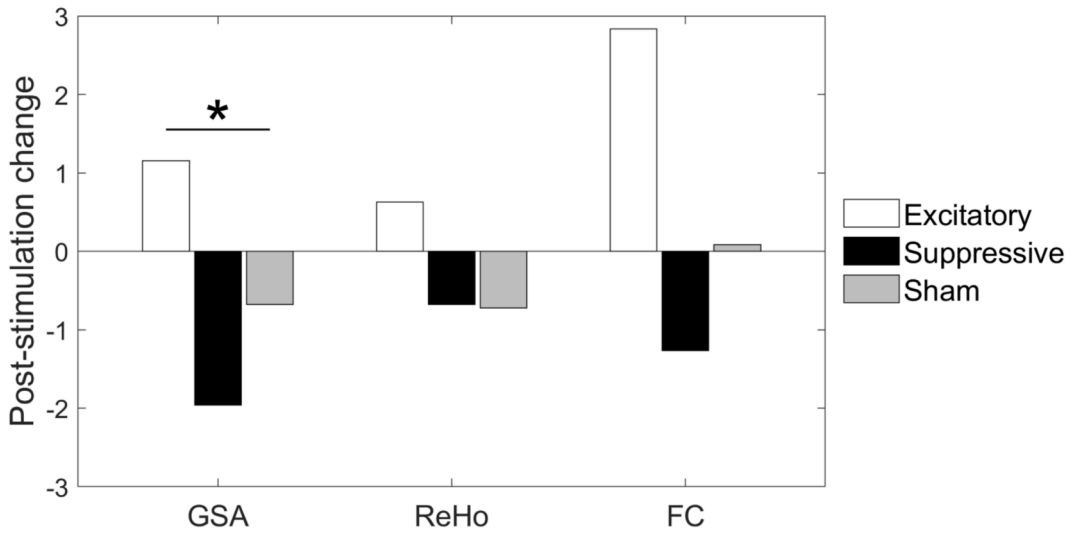


Fig. 3. Changes in (A) global signal amplitude (GSA), (B) regional homogeneity (ReHo), and (C) inter-regional functional connectivity (FC) after transcranial focused ultrasound. Positive and negative values indicate increases and decreases in each measure, respectively. Changes in each measure were rescaled according to their standard deviation to allow for direct comparison while maintaining their original mean. A significant differences among three groups is indicated by an asterisk.

persisted when individually comparing excitatory and suppressive stimulations against sham stimulation, and it was more pronounced when comparing excitatory stimulation directly with suppressive stimulation (Fig. 6 and Table S3).

3.5. Network-wise changes in structure–function correspondences

At the level of each cerebral network, changes in structure–function correspondences were characteristically observed as increased coupling between structure and function only under excitatory stimulation (Fig. 7 and Table 2): structure and function were coupled more strongly across the visual and limbic networks and significantly more strongly coupled across the DMN. When comparing excitatory stimulation with suppressive stimulation, as well as with sham stimulation, the increased structure–function correspondence under excitatory stimulation persisted only for the DMN (Fig. 8 and Table 2), implying that changes in structure–function correspondences across cerebral networks other than the DMN were limited.

3.6. Changes in structure–function correspondences across the default mode network

Upon closer examination of the changes in structure–function correspondences across the DMN (Fig. 9), both the excitatory and suppressive stimulations elicited pronounced increases in the medial orbital part of the SFG, but the extent of change under excitatory stimulation encompassed the dorsolateral and medial parts of the SFG and even reached the anterior cingulate and paracingulate gyri, providing more widespread alterations across the DMN than the suppressive stimulation. However, the changes induced by excitatory stimulation did not propagate to the posterior cingulate gyrus or the parietal and temporal cortices, indicating that the modulation was confined to the anterior portions of the DMN.

4. Discussion

For this work, we investigated how low-intensity tFUS with various sonication parameters targeting the mPFC modulates brain networks, particularly the DMN. We measured changes in structure–function correspondences as a surrogate for brain state changes following tFUS, and found that excitatory tFUS stimulation specifically modulated the DMN connected to the mPFC, whereas the modulatory effects of suppressive tFUS stimulation remained unclear. Our findings highlight the capacity of tFUS to effectively modulate the DMN depending on sonication parameters.

Although targeting the mPFC as the stimulation site appears to be one of the earliest attempts, our choice of the mPFC aimed to modulate the DMN beyond the mPFC. In other words, we ultimately targeted the DMN through its connectivity with the stimulation site, which is in alignment with recent interest in the principle of targeting brain circuits to treat various neuropsychiatric disorders (Siddiqi et al., 2024). While we hypothetically selected the mPFC as the stimulation site to target the DMN, more systematic methods for determining stimulation sites are needed.

Compared to the recent literature based on tFUS of the posterior cingulate cortex (Lord et al., 2024), modulation using our approach targeting the mPFC was confined to the anterior brain regions and did not reach significant changes in other regions, including the parietal and temporal cortices, future studies should investigate which of the brain regions could be the key components of impacts on the DMN for specific neuromodulation effects. In our experimental paradigm focused on short-term brain changes following tFUS stimulation, we hypothesized that the structural properties of the brain would remain stable while functional dynamics would exhibit measurable alterations. Indeed, resting-state fMRI analyses revealed that functional activity and connectivity, as indexed by GSA, ReHo, and FC, generally increased following excitatory stimulation and decreased following suppressive stimulation, aligning with our expectations of protocol-specific effects. However, these changes were not consistently robust, particularly at the network level, where identify specific network-related changes proved challenging. This limitation highlights the challenge of detecting subtle neuromodulatory effects using fMRI measures alone. Consequently, in this study, we further explored the structure–function correspondence as a potentially more sensitive measure to capture stimulation-induced changes in brain dynamics.

While we observed increased structure-function correspondence in the DMN following tFUS, its functional significance warrants careful interpretation. Based on previous research demonstrating associations between higher baseline correspondence and improved learning outcomes (Park et al., 2024), our findings might suggest that tFUS induces a more optimized state for subsequent functional processing, but this interpretation remains speculative at present. The direct implication of tFUS-induced changes in the structure-function correspondence for DMN-related functions need to be established through future studies

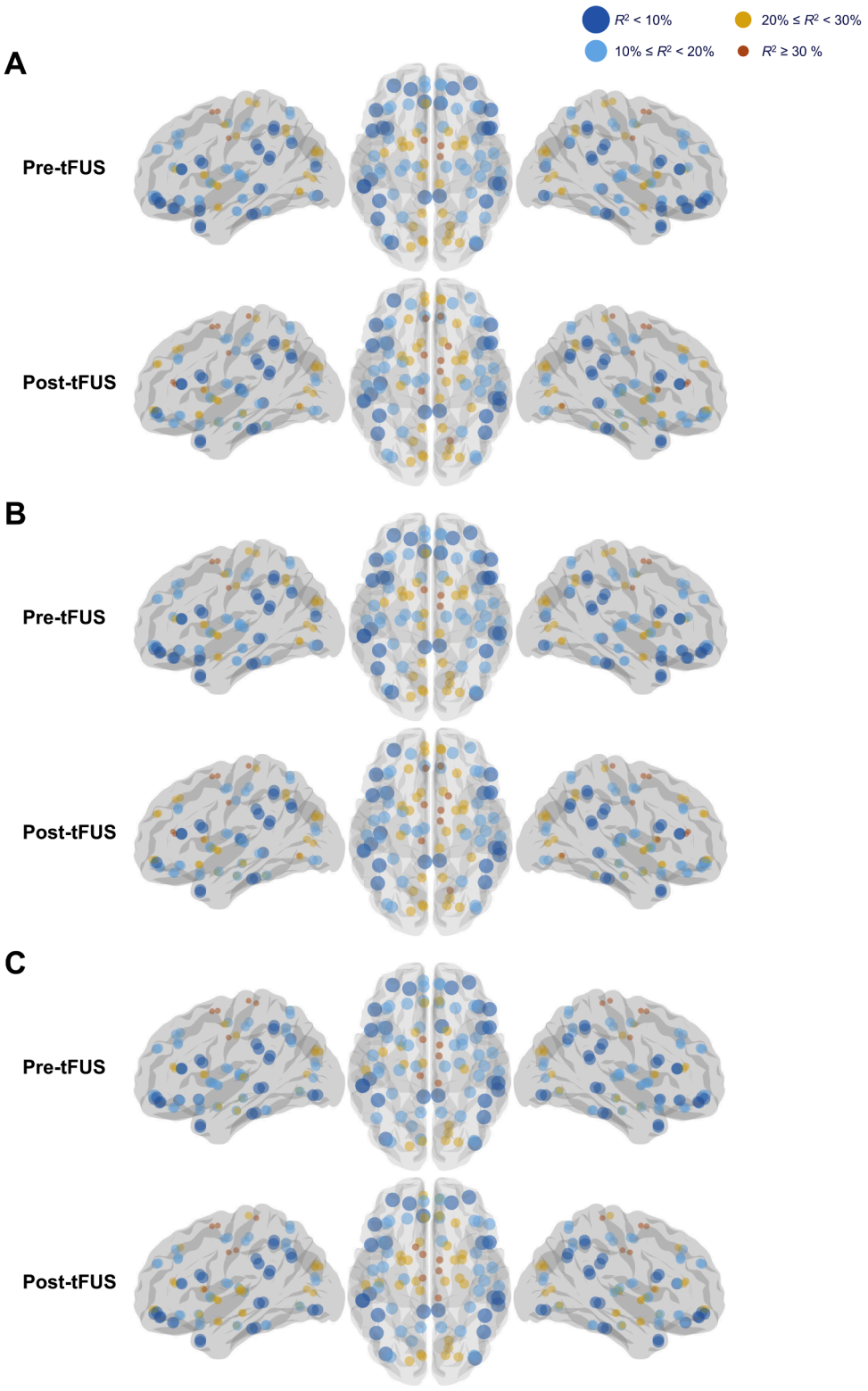


Fig. 4. Distribution of structure-function correspondence values across the cerebral cortex before (pre-tFUS) and after transcranial ultrasound (post-tFUS) for (A) excitatory, (B) suppressive, and (C) sham stimulations. Color scale represents R^2 values indicating the strength of structure-function correspondence at each brain area.

incorporating behavioral measures and larger sample sizes.

Our results demonstrate the sonication parameter-dependent nature of tFUS effects. Modulation of the DMN, manifested as increased structure–function correspondence, was successfully accomplished using the excitatory stimulation protocol but not the suppressive stimulation protocol. This protocol-dependent effect adds to the growing literature on DMN modulation through tFUS, such as the recent work demonstrating successful DMN modulation using tFUS of the posterior cingulate cortex (Lord et al., 2024). The differential effects observed across studies using various protocols and targets within the DMN underscore

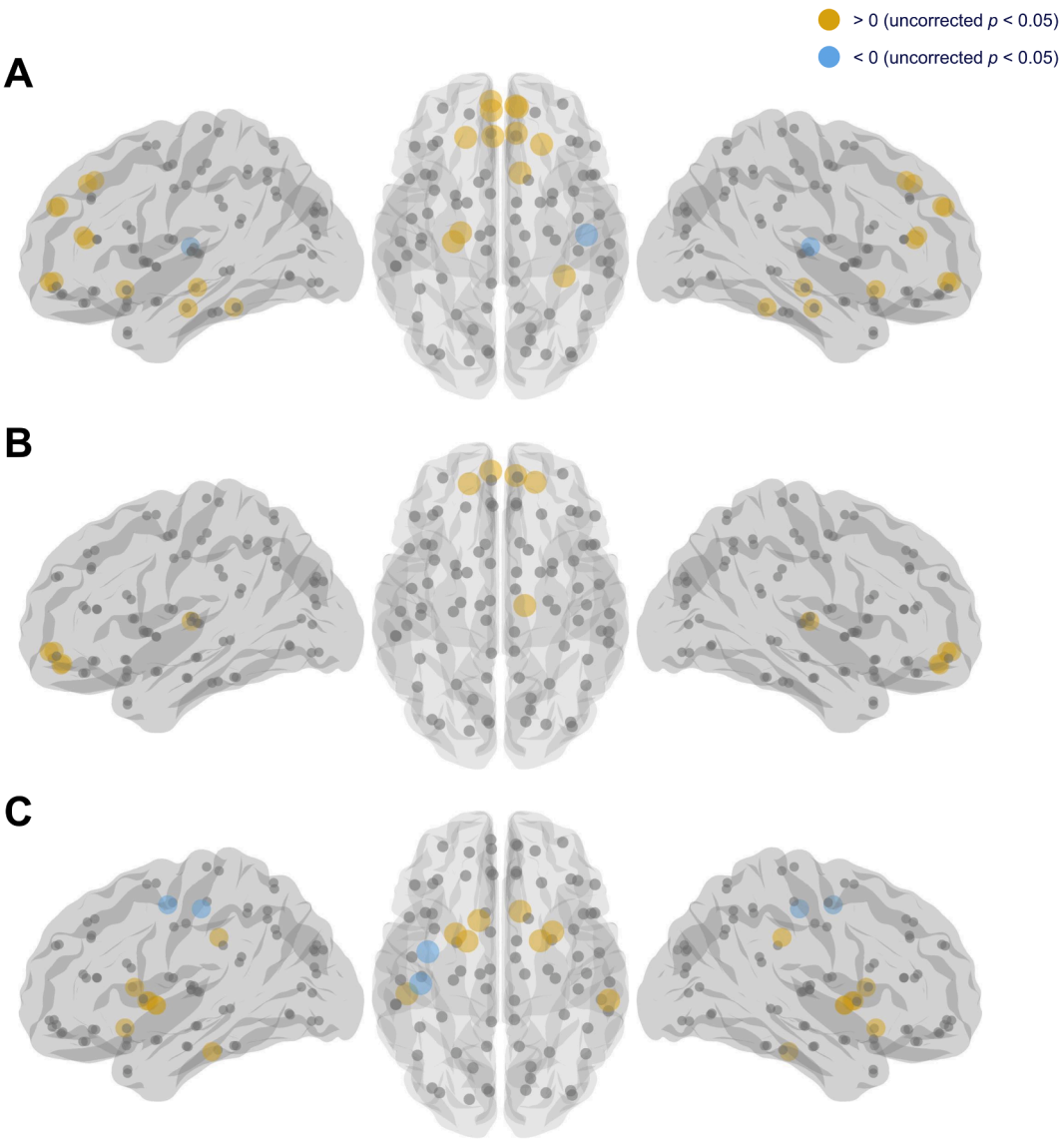


Fig. 5. Node-wise changes in structure-function correspondence following transcranial focused ultrasound for (A) excitatory, (B) suppressive, and (C) sham stimulations. Brain maps show changes compared to baseline, with warm colors indicating significant increases and cool colors indicating significant decreases.

the importance of systematic investigation of stimulation parameters to advance our understanding of tFUS-induced neuromodulation. Furthermore, while the excitatory stimulation protocol proposed in this study demonstrated the expected effects, detailed characterization of acoustic energy delivery and systematic investigation of various duty cycles are essential for further tuning and optimization of therapeutic tFUS applications for neuropsychiatric disorders. Future studies should incorporate comprehensive intensity measurements with empirical validation of computational models to enhance our understanding of the relationship between sonication parameters and neuromodulatory effects.

The absence of adverse effects reported in this study validates the utility of tFUS as a safe method for neuromodulation. This safety profile, combined with the observed modulatory effects of the DMN, indicates the potential of tFUS for neurotherapeutic applications. Our primary motivation for tFUS application to the mPFC to modulate the DMN stems from its potential to enhance the therapeutic efficacy of neuropsychiatric disorders associated with DMN dysfunction (for reviews, see (Broyd et al., 2009; Mohan et al., 2016)). Given that the mechanisms linking DMN dysfunction to various disorders appear to be diverse (Broyd et al., 2009), the approaches needed for effective DMN modulation could vary according to the type of the specific disorder, and even the stage of its progression. Although further research is required to address these concerns, our findings demonstrate that tFUS offers distinct technical advantages for modulating deep brain circuits such as the DMN, particularly through its ability to deliver focused stimulation to deep structures with millimeter-scale spatial resolution, combined with its established safety profile. While these capabilities have been essential for targeted modulation of the mPFC, we acknowledge that various neuromodulation approaches may be optimal for specific experimental and clinical applications.

The main limitation of this study was the relatively small sample size. Our goal here, however, was to compare stimulation protocols to determine the most effective one in order to evaluate the actual impact of tFUS on subsequent brain functional or behavioral changes. Therefore, we sought to minimize the number of participants for each protocol, which limits statistical powers but is sufficient for preliminary purposes for the future clinical investigations. Future research should verify whether the findings of this study can be generalized in larger samples or specific clinical situations.

The second limitation involves the lack of long-term follow-up to assess the durability of tFUS-induced changes. The DMN modulation

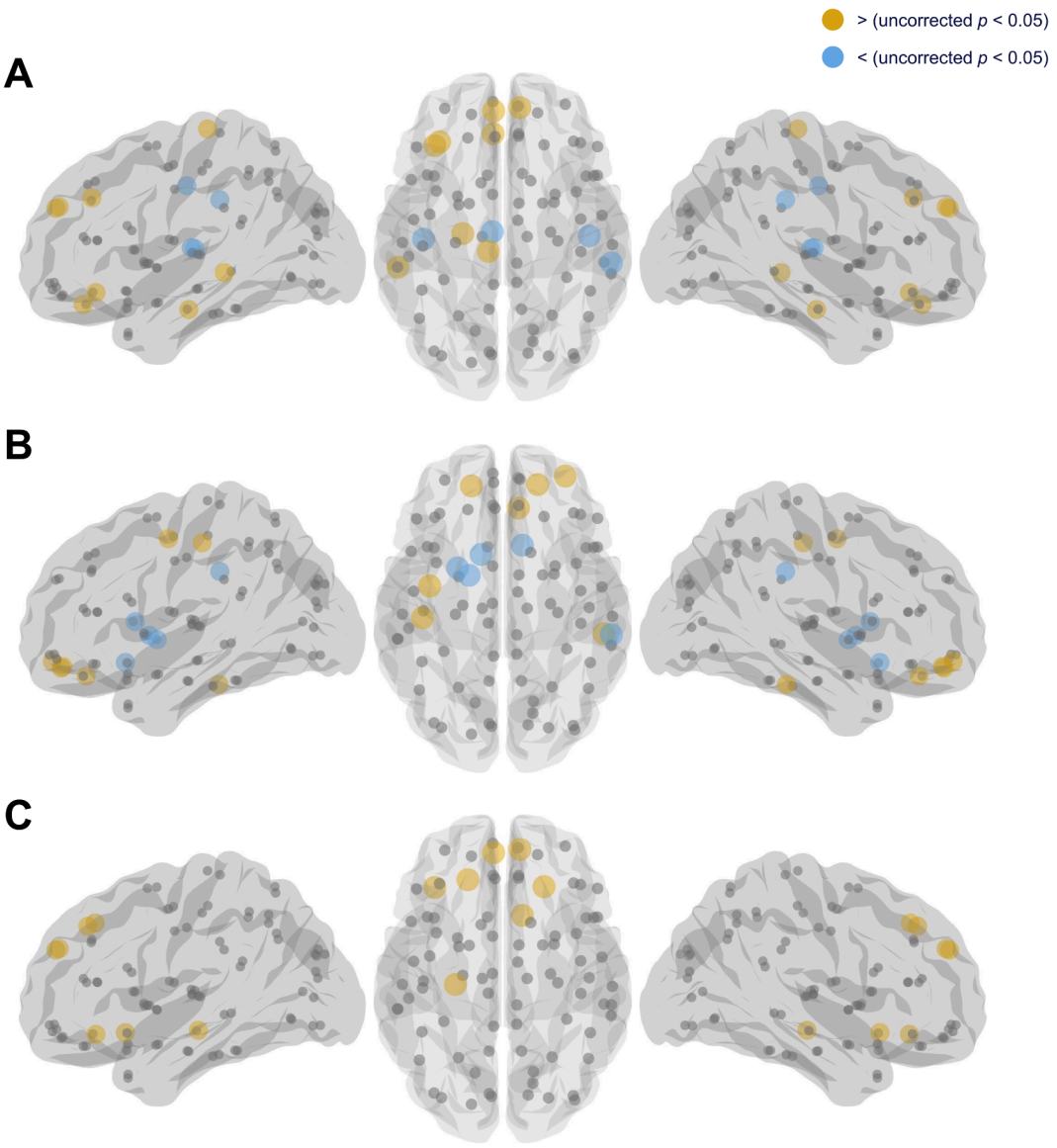


Fig. 6. Between-group comparison of node-wise changes in structure-function correspondence following focused ultrasound. Brain maps show differences in changes between (A) excitatory vs. sham, (B) suppressive vs. sham, and (C) excitatory vs. suppressive stimulations, with warm and cool colors indicating significantly larger and smaller changes, respectively, for the former than the latter of each comparison pair.

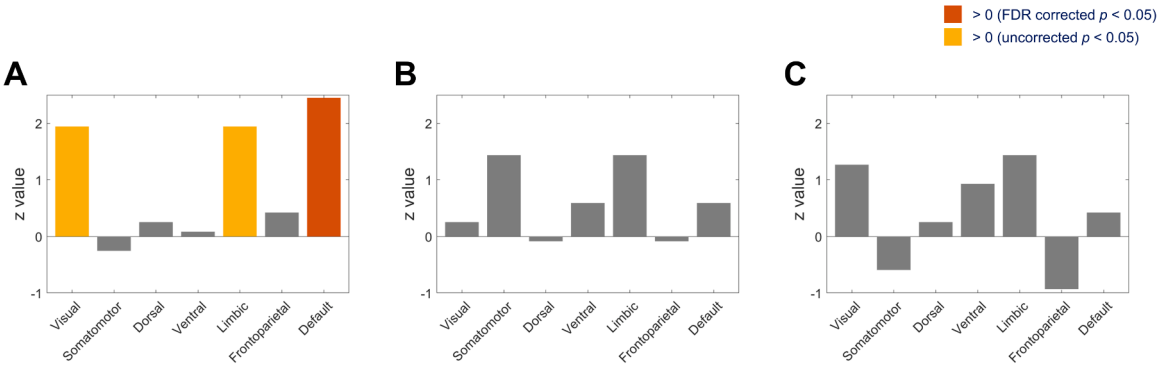


Fig. 7. Network-wise changes in structure–function correspondence following transcranial focused ultrasound for (A) excitatory, (B) suppressive, and (C) sham stimulations. Positive and negative z-values represent increases and decreases in structure–function correspondence, respectively, with color coding indicating statistical significance.

Table 2
Network-wise changes in structure–function correspondences after excitatory transcranial focused ultrasound (tFUS) stimulation. Statistical significance after correction for multiple comparisons is indicated in bold.

(A) Increase after excitatory tFUS			
Inference	Cerebral network	*Z*-value	*P*-value
> 0	Default mode	2.282	0.011
	Visual	1.775	0.038
	Limbic	1.775	0.038

(B) Larger change after excitatory tFUS than after sham tFUS			
Inference	Cerebral network	*Z* value	*P*-value
>	Default mode	2.044	0.020

(C) Larger change after excitatory tFUS than after suppressive tFUS			
Inference	Cerebral network	*Z* value	*P* value
>	Default mode	1.661	0.048

observed in this study represents acute changes following a single session of tFUS administration. Future studies are needed to investigate both the duration of these effects, potential plasticity mechanisms, and whether these neural changes translate into behavioral outcomes.

5. Conclusions

In this study, we aimed to target and modulate the DMN by selecting the mPFC as the stimulation site for tFUS. We demonstrated the modulating effects of tFUS on the DMN in terms of increases in structure–function correspondences across relevant brain areas beyond the mPFC. Furthermore, those modulatory effects varied depending on specific sonication parameters. These findings contribute to a deeper understanding of tFUS as a neuromodulation tool, paving the way for its integration into neuroscience research and clinical practice. Future studies should focus on elucidating the long-term effects of tFUS and refining sonication parameters to enable more effective modulation.

CRediT authorship contribution statement

Chang-hyun Park: Writing – original draft, Formal analysis. **Song E. Kim:** Writing – review & editing, Validation, Methodology, Investigation, Formal analysis, Data curation. **Yun Seo Choi:** Writing – review & editing, Visualization, Investigation. **Jihye Lee:** Formal analysis, Investigation, Writing – review & editing. **Seo Young Lee:** Writing – review & editing, Methodology, Formal analysis. **Ju Hyeong Kang:** Writing – review & editing, Investigation, Formal analysis. **Seongeun Hwang:** Writing – review & editing, Validation, Investigation, Data curation. **Young Goo Kim:** Writing – review & editing, Validation,

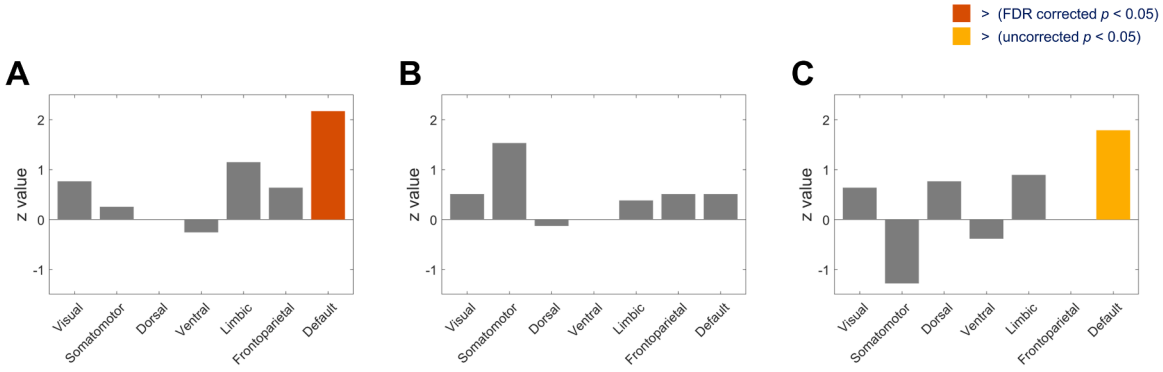


Fig. 8. Between-group comparisons of network-wise changes in structure–function correspondence following transcranial ultrasound. Positive or negative z-values represent differences in changes between (A) excitatory vs. sham, (B) suppressive vs. sham, and (C) excitatory vs. suppressive stimulations, with positive and negative z-values representing larger and smaller changes, respectively, for the former than the latter of each comparison pair and color coding indicating statistical significance.

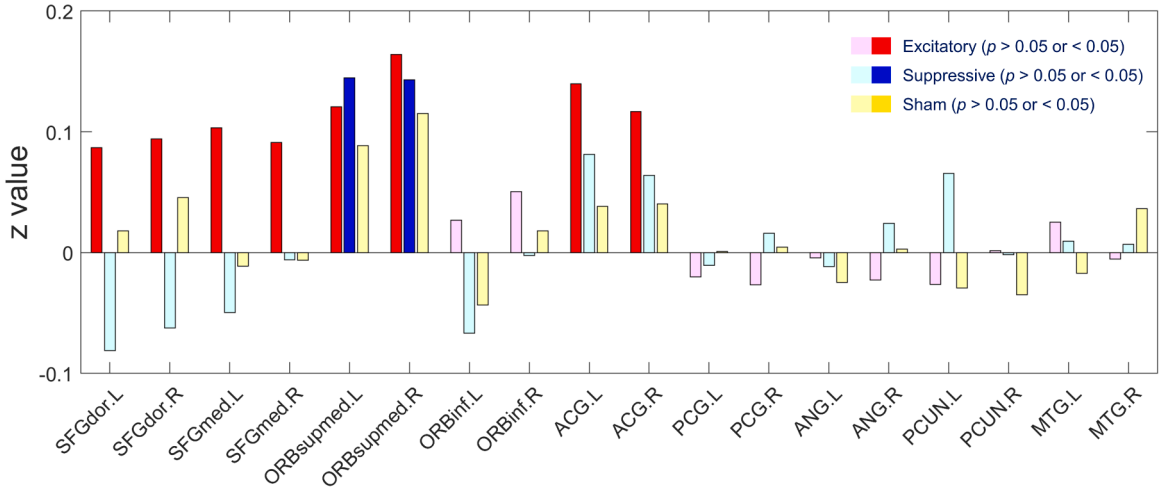


Fig. 9. Node-wise changes in structure–function correspondences across brain areas comprising the default mode network following transcranial focused ultrasound for different stimulation conditions. Positive and negative z-values represent increases and decreases in structure-function correspondence, respectively, with color coding indicating statistical significance.

Investigation, Data curation. **Hyang Woon Lee:** Writing – review & editing, Supervision, Investigation, Funding acquisition, Formal analysis, Data curation, Conceptualization.

Declaration of competing interest

The authors have no conflict of interests to disclose.

Acknowledgements

This study was supported by RP-Grant 2022 and 2023 of Ewha Womans University to S.E.K., grants from the Korea Health Technology R&D Project through the Korea Health Industry Development Institute (KHIDI), funded by the Ministry of Health & Welfare (RS-2023-KH139976 to S.H., H.W.L.; RS-2024–00440131 to Y.G.K., and H.W.L.), the Bio-Core Facility Construction Project, the Bio & Medical Technology Development of the National Strategic R&D Project (RS-2022-NR067387, RS-2023-00265524, and RS-2025–02218624) and BK21 Plus Programs through the National Research Foundation of Korea to H. W.L., and the Institute of Information & communications Technology Planning & Evaluation (IITP) grant (No. RS-2022–00155966) by the Korean government (MSIT) to C.P. and H.W.L., and the Artificial Intelligence Convergence Innovation Human Resources Development programs of Ewha Womans University to H.W.L.

Supplementary materials

Supplementary material associated with this article can be found, in the online version, at doi:10.1016/j.neuroimage.2025.121540.

Data availability

Data will be made available upon reasonable request.

References

Beisteiner, R., 2022. Human ultrasound neuromodulation: state of the art. Brain Sci. 12, 208.
Beisteiner, R., Matt, E., Fan, C., Baldysiak, H., Schönfeld, M., Philippi Novak, T., Amini, A., Aslan, T., Reinecke, R., Lehrner, J., 2020. Transcranial pulse stimulation with ultrasound in Alzheimer's disease—a new navigated focal brain therapy. Adv. Sci. 7, 1902583.
Broyd, S.J., Demanuele, C., Debener, S., Helps, S.K., James, C.J., Sonuga-Barke, E.J., 2009. Default-mode brain dysfunction in mental disorders: a systematic review. Neurosci. Biobehav. Rev. 33, 279–296.
Clement, G.T., Hynynen, K., 2002. A non-invasive method for focusing ultrasound through the human skull. Phys. Med. Biol. 47, 1219.
Dell'Italia, J., Sanguinetti, J.L., Monti, M.M., Bystritsky, A., Reggente, N., 2022. Current state of potential mechanisms supporting low intensity focused ultrasound for neuromodulation. Front. Hum. Neurosci. 16, 872639.
Griffa, A., Amico, E., Liégeois, R., Van De Ville, D., Preti, M.G., 2022. Brain structure-function coupling provides signatures for task decoding and individual fingerprinting. Neuroimage 250, 118970.
Jeurissen, B., Tournier, J.-D., Dhollander, T., Connelly, A., Sijbers, J., 2014. Multi-tissue constrained spherical deconvolution for improved analysis of multi-shell diffusion MRI data. Neuroimage 103, 411–426.
Kim, Y.G., Kim, S.E., Lee, J., Hwang, S., Yoo, S.S., Lee, H.W., 2022. Neuromodulation using transcranial focused ultrasound on the bilateral medial prefrontal cortex. J. Clin. Med. 11, 3809.
Kubanek, J., 2018. Neuromodulation with transcranial focused ultrasound. Neurosurg. Focus 44, E14.
Legon, W., Adams, S., Bansal, P., Patel, P.D., Hobbs, L., Ai, L., Mueller, J.K., Meekins, G., Gillick, B.T., 2020. A retrospective qualitative report of symptoms and safety from transcranial focused ultrasound for neuromodulation in humans. Sci. Rep. 10, 5573.
Lord, B., Sanguinetti, J.L., Ruiz, L., Miskovic, V., Segre, J., Young, S., Fini, M.E., Allen, J. J., 2024. Transcranial focused ultrasound to the posterior cingulate cortex modulates default mode network and subjective experience: an fMRI pilot study. Front. Hum. Neurosci. 18, 1392199.
Martin, E., Aubry, J.F., Schafer, M., Verhagen, L., Treeby, B., Pauly, K.B., 2024. ITRUSST consensus on standardised reporting for transcranial ultrasound stimulation. Brain Stimul. 17, 607–615.
Mohan, A., Roberto, A.J., Mohan, A., Lorenzo, A., Jones, K., Carney, M.J., Liogier-Weyback, L., Hwang, S., Lapidus, K.A., 2016. Focus: the aging brain: the significance of the default mode network (DMN) in neurological and neuropsychiatric disorders: a review. Yale J. Biol. Med 89, 49.
Monti, M.M., Schnakers, C., Korb, A.S., Bystritsky, A., Vespa, P.M., 2016. Non-invasive ultrasonic thalamic stimulation in disorders of consciousness after severe brain injury: a first-in-man report. Brain Stimul. 9, 940–941.
Oh, J., Ryu, J.S., Kim, J., Kim, S., Jeong, H.S., Kim, K.R., Kim, H.-C., Yoo, S.-S., Seok, J.-H., 2024. Effect of Low-Intensity transcranial focused ultrasound stimulation in patients with major depressive disorder: A randomized, Double-Blind, Sham-Controlled Clinical Trial. Psych. Investig. 21, 885–896.
Park, C.H., Durand-Ruel, M., Moyne, M., Morishita, T., Hummel, F.C., 2024. Brain connectome correlates of short-term motor learning in healthy older subjects. Cortex 171, 247–256.
Raichle, M.E., 2015. The brain's default mode network. Annu. Rev. Neurosci. 38, 433–447.
Reznik, S.J., Sanguinetti, J.L., Tyler, W.J., Daft, C., Allen, J.J., 2020. A double-blind pilot study of transcranial ultrasound (TUS) as a five-day intervention: TUS mitigates worry among depressed participants. Neurol Psychiatry Brain Res. 37, 60–66.
Sarica, C., Nankoo, J.-F., Fomenko, A., Grippe, T.C., Yamamoto, K., Samuel, N., Milano, V., Vetkas, A., Darmani, G., Cizmeci, M.N., Lozano, A.M., Chen, R., 2022. Human Studies of Transcranial ultrasound neuromodulation: a systematic review of effectiveness and safety. Brain Stimul. 15, 737–746.
Siddiqi, S.H., Khosravani, S., Rolston, J.D., Fox, M.D., 2024. The future of brain circuit-targeted therapeutics. Neuropsychopharmacology 49, 179–188.
Smallwood, J., Bernhardt, B.C., Leech, R., Bzdok, D., Jefferies, E., Margulies, D.S., 2021. The default mode network in cognition: a topographical perspective. Nat. Rev. Neurosci. 22, 503–513.
Stern, J.M., Spivak, N.M., Becerra, S.A., Kuhn, T.P., Korb, A.S., Kronemyer, D., Khanlou, N., Reyes, S.D., Monti, M.M., Schnakers, C., 2021. Safety of focused ultrasound neuromodulation in humans with temporal lobe epilepsy. Brain Stimul. 14, 1022–1031.
Tournier, J.-D., Smith, R., Raffelt, D., Tabbara, R., Dhollander, T., Pietsch, M., Christiaens, D., Jeurissen, B., Yeh, C.-H., Connelly, A., 2019. MRtrix3: a fast, flexible and open software framework for medical image processing and visualisation. Neuroimage 202, 116137.
Tzourio-Mazoyer, N., Landeau, B., Papathanassiou, D., Crivello, F., Etard, O., Delcroix, N., Mazoyer, B., Joliot, M., 2002. Automated anatomical labeling of activations in SPM using a macroscopic anatomical parcellation of the MNI MRI single-subject brain. Neuroimage 15, 273–289.
Vázquez-Rodríguez, B., Suárez, L.E., Markello, R.D., Shafiei, G., Paquola, C., Hagmann, P., Van Den Heuvel, M.P., Bernhardt, B.C., Spreng, R.N., Misic, B., 2019. Gradients of structure–function tethering across neocortex. Proc. Natl. Acad. Sci. 116, 21219–21227.
Yeo, B.T., Krienen, F.M., Sepulcre, J., Sabuncu, M.R., Lashkari, D., Hollinshead, M., Roffman, J.L., Smoller, J.W., Zöllei, L., Polimeni, J.R., 2011. The organization of the human cerebral cortex estimated by intrinsic functional connectivity. J. Neurophysiol.
Zhang, T., Pan, N., Wang, Y., Liu, C., Hu, S., 2021. Transcranial focused ultrasound neuromodulation: a review of the excitatory and inhibitory effects on brain activity in Human and animals. Front. Hum. Neurosci. 15.